ACS Macro Letters

Letter

pubs.acs.org/macroletters

Crystallization-Induced Hybrid Nano-Sheets of Fluorescent Polymers with Aggregation-Induced Emission Characteristics for Sensitive Explosive Detection

Guodong Liang,[†,‡,§] Lu-Tao Weng,[∥] Jacky W. Y. Lam,[†,‡] Wei Qin,[†,‡] and Ben Zhong Tang*[,†,‡,⊥]

[†]HKUST-Shenzhen Research Institute, No. 9 Yuexing first RD, South Area, Hi-tech Park, Nanshan, Shenzhen, China 518057

[‡]Department of Chemistry, Institute for Advanced Study, Division of Biomedical Engineering, Institute of Molecular Functional Materials, The Hong Kong University of Science and Technology, Clear Water Bay, Kowloon, Hong Kong, China

[§]DSAP lab, PCFM lab, School of Chemistry and Chemical Engineering, Sun Yat-Sen University, Guangzhou 510275, China

[∥]Materials Characterization and Preparation Facility, Department of Chemical and Biomolecular Engineering, The Hong Kong University of Science and Technology, Hong Kong, China

[⊥]Guangdong Innovative Research Team, SCUT-HKUST Joint Research Laboratory, State Key Laboratory of Luminescent Materials and Devices, South China University of Technology, Guangzhou 510640, China

Supporting Information

ABSTRACT: Fluorescent organic hybrid nanosheets were generated by crystallization of polymers capped with luminogenic molecules exhibiting aggregation-induced emission characteristics (AIE). During crystallization of polymers, AIE molecules were expelled out of lamellar crystals of polymers, and finally resided on the surface. The fluorescent nanosheets with dangling AIE molecules showed sensitive and specific response to explosives. Such polymer crystallization-induced fluorescent nanomaterials offers a unique avenue to fabricate functional nanomaterials with AIE molecule-enriched domains for potential applications in nanodevices, biological engineering, and so on.

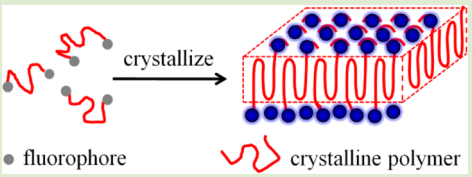

Fluorescent nanomaterials with aggregation-induced emission characteristics (AIE) are emerging as a class of promising materials. Taking advantage of high quantum yield of AIE molecules, AIE nanomaterials emit efficiently in the solid state, which results in a broad range of applications in photonics, nanodevices, biological engineering, and so on.[1]

To date, fluorescent nanomaterials with varied morphologies including rods and ribbons have been synthesized through self-assembly of fluorescent molecules.[2] The small molecules aligned regularly to form ordered nanostructures driven by crystallization, hydrogen bonding, hydrophobic interaction, and so on. Fluorescence properties of nanostructures are dependent on the packing and aggregation structure of fluorescent molecules due to interaction among adjacent molecules.[3] Tuning alignment and aggregation of fluorescent molecules is crucial for fundamentally understanding the fluorescence mechanism and also important for optimizing fluorescence properties. So far, tuning the alignment of fluorescent molecules in a controlled fashion remains challenging, likely due to the lack of proper approach.

Crystallization is regarded as a naturally occurring self-assembly process. Polymer chains fold up and arrange regularly into lamellae of about 10 nm in thickness during crystallization.[4] This offers a new opportunity for tuning the alignment of fluorescent molecules, affording a kind of hybrid fluorescent nanomaterials with functional molecule-enriched domains. In this respect, hybrid fluorescent materials consisted of multiple components take advantage of each component, showing advanced overall performances.[5] However, polymer crystallization-induced formation of fluorescent nanomaterials is unprecedented to our best knowledge.

Herein we reported a general approach for tuning the alignment of fluorescent molecules by crystallization of polymers, affording a class of fluorescent hybrid nanomaterials. Crystallizable polymers capped with AIE molecules were allowed to crystallize. During crystallization of polymers, AIE molecules were excluded out of polymer lamellar crystals and finally located to the surface of lamellae, as illustrated in Scheme 1. We demonstrated that with exposed AIE molecules, the fluorescent hybrid nanosheets showed sensitive response to model explosive of picric acid.

Poly(ε-caprolactone) was selected as crystalline polymer due to its high crystallinity, superior solubility, and broad applications in biological engineering.[6] A typical AIE molecule of tetraphenylethene (TPE) was utilized as a luminogenic molecule because of its high quantum yield and its distinct chemical structure compared to the polymer backbone.[7] It is expected that this difference in chemical structure between the polymer backbone and the TPE would make the TPE to be

Received: November 13, 2013
Accepted: December 11, 2013
Published: December 13, 2013

Scheme 1. Schematic Illustration of Crystallization-Induced Nano-Sheets of Fluorescent Polymers

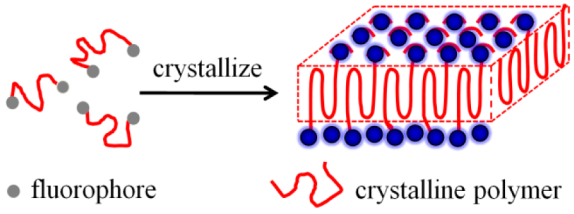

preferentially segregated out during the PCL crystallization. Poly(ε-caprolactone) terminated with tetraphenylethene (PCL-TPE) was synthesized by condensation reactions between PCL and monocarboxylic acid-substituted TPE (TPE-CO_2H; Schemes S1 and S2). Detailed procedures for the synthesis of PCL-TPE were described in the Supporting Information (SI). All the intermediates and desirable products were characterized by NMR and mass spectrometry and obtained satisfactory results corresponding to their molecular structures (Figures S1−S7, SI). The number average molecular weight of PCL-TPE was 3.5 kg/mol with distribution of 1.15. The number of repeating units of PCL was 28 and the weight percentage of TPE units in PCL-TPE was 4.3 wt % (Table S1, SI).

Crystallization and melting behaviors of PCL-TPE were investigated using differential scanning calorimetry (DSC; Figures S8 and S9 and Table S2, SI). PCL-TPE showed a distinct exothermic peak at 37.2 °C in cooling scan, ascribed to crystallization of PCL. A sharp endothermic peak at 52.3 °C was observed in the subsequent heating scan stemming from melting of PCL crystals.[8] The degree of crystallinity of PCL-TPE was estimated to be 55.9%. These data showed that PCL-TPE was crystallizable, as expected.

PCL-TPE emitted efficiently in the solid state, while radiated weakly when dissolved in a good solvent such as THF. We therefore investigated fluorescence behaviors of PCL-TPE in THF/H_2O mixture, as revealed in Figure 1. PCL-TPE emitted

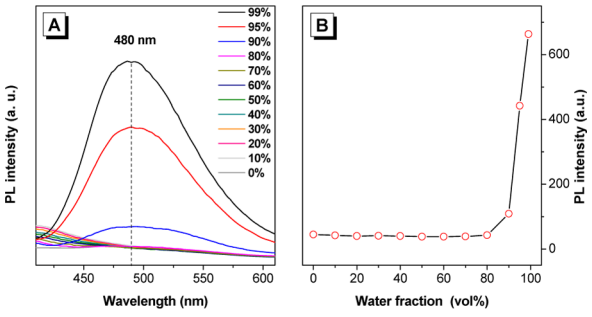

Figure 1. (A) PL spectra of PCL-TPE in THF/H_2O mixture at various water fractions and (B) variation of fluorescence intensity at 480 nm against water fractions. Radiation: 350 nm.

weakly in the THF/H_2O mixture at low water fractions ($\leq$80 vol%). The intensity of emission at 480 nm increased abruptly with increasing water fraction to 99 vol%, revealing a typical aggregation-induced emission (AIE) phenomenon.[1]

Morphology of PCL-TPE suspended in aqueous media was characterized using atomic force microscopy (AFM). Height image of tapping mode AFM revealing lamellar structures of PCL-TPE was shown in Figure 2. Cross-sectional profile showed that the thickness of sheets was approximately 7.0 nm, close to the thickness of PCL lamellar crystals.[8] To investigate

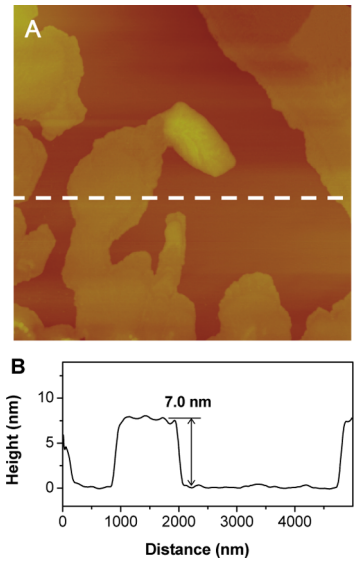

Figure 2. (A) Height image of tapping mode AFM of PCL-TPE and (B) cross-sectional profile along the white dashline. Image size: 5 × 5 μm^2.

the microstructure of PCL-TPE nanosheets, the PCL-TPE nanosheet powders were isolated by centrifuging and filtration of PCL-TPE suspension. XRD spectrum of PCL-TPE nanosheets showed two distinct diffraction peaks at 21.3° and 23.6° associated with (110) and (200) diffraction plane of PCL orthorhombic crystals, respectively, indicating that PCL crystallized (Figure S10, SI). A sharp endothermic peak observed in the DSC trace in the first heating scans further confirmed crystallization of PCL-TPE (Figure S11, SI).

Surface composition of PCL-TPE lamellae was analyzed using a very surface sensitive technique: time-of-flight secondary ion mass spectrometry (TOF-SIMS). The sampling depth of TOF-SIMS is typically 1−2 nm for molecular ions, depending on the primary ions used.[9] A typical positive TOF-SIMS spectrum of PCL-TPE using Bi_3^+ as primary ion beam was shown in Figure S12. The fragments from both PCL backbone and TPE end groups were detected. In particular, the fragment at m/z = 115 ($C_6H_{11}O_2^+$) represented the repeat unit of PCL, while the fragment at m/z = 357 ($C_{27}H_{17}O^+$) was ascribed to the TPE moieties (Table S3).

To determine whether the TPE was on the surface, the results obtained with two different primary ion beams (Bi_3^+ and C_{60}^+) were compared as it has been shown that sampling depth is dependent on the size of primary ion beams under identical ion dosage. Smaller size ion beam will provide a deeper sampling depth.[9a,b] The TOF-SIMS spectrum of PCL-TPE using C_{60}^+ as primary ion beam (Figure S13, SI) was similar to that using Bi_3^+ (Figure S12). However, the peak intensities of fragments from polymer backbone and TPE moiety are different. For example, the TOF-SIMS intensity ratio between the peak at m/z = 357 and that at m/z = 115 (I_{357}/I_{115}) was 1.9 × 10^{-2} when using Bi_3^+ as primary ion beam, which is by far lower than that using C_{60}^+ as primary ion beam (17.5 × 10^{-2}). This revealed that TPE fractions decreased drastically with increasing sampling depth, suggesting that TPE moieties are located on the surface of PCL-TPE nanosheets.

To confirm the above conclusion, TOF-SIMS spectra were obtained at various temperatures using C_{60}^+ as primary ion beam. Figure 3 displayed the intensity ratio I_{357}/I_{115} as a

dx.doi.org/10.1021/mz4005887 | ACS Macro Lett. 2014, 3, 21−25

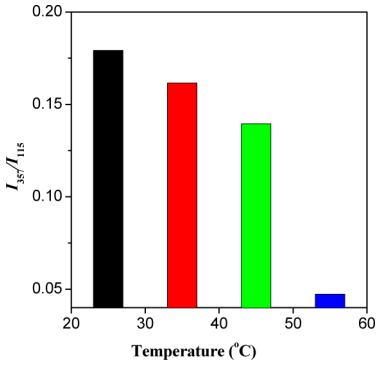

Figure 3. TOF-SIMS intensity ratio (I_{375}/I_{115}) as a function of temperature.

function of temperature. It clearly showed that the TPE concentration started to slightly decrease from 35 °C and decrease abruptly after the melting temperature of PCL-TPE (52.3 °C). At 55 °C (Figure S14; ESI), the intensity ratio is about 1/4 of that obtained on PCL-TPE lamellae (25 °C). This is expected as at 55 °C the PCL-TPE lamellae were melted and the end groups (TPE moieties) should be randomly distributed across the whole polymer film.[9b] As a result, the surface TPE concentration at molten state is much lower compared to that of lamellae. Based on ToF-SIMS results, the grafting density of TPE moieties was estimated to be 3.9×10^{17} m^{-2} (SI).

X-ray photoelectron spectroscopy (XPS) measurements at two different sampling depths were also carried out on the same sample. Only carbon and oxygen were detected by XPS. At a takeoff angle of 45° (corresponding to a sampling depth of ~5 nm[9c]), the oxygen fraction of PCL-TPE lamellae was determined to be 20.1%, which is lower than the theoretical concentration of pure PCL (25%). This implies that there are oxygen-deficient TPE moieties on the surface. At a takeoff angle of 25° (sampling depth ~3 nm[9c]), the oxygen fraction decreased to 16.5% (Figure S15, SI). These results further supported that the TPE moieties resided on the surface of PCL-TPE lamellae, in agreement with the TOF-SIMS results.

The above TOF-SIMS and XPS results imply that during the crystallization of PCL segments, the end groups of TPE are expelled out of PCL crystals. This results in TPE dangling on the surface due to being covalently bonded to polymers. Two possible reasons account for the exposed TPE moieties on polymer lamellae: (1) size of bulky TPE moieties does not match with PCL crystal cell[10] (a = 0.748 nm, b = 0.498 nm, c = 1.726 nm; Figure S16); (2) low miscibility between the nonpolar aromatic TPE moieties and the polar aliphatic caprolactone segments. As a matter of fact, there are no reports that end groups can be trapped inside polymer lamellae to date. Even small end groups such as thiol, hydroxide, carboxyl acid, and benzyl, cannot enter lamellae and locate to the surface of lamellae.[11] In the case of polymers with a bromine as the end group, the Br distribution has been monitored using TOF-SIMS during polymer crystallization and the results clearly showed that the Br groups were expelled to the surface of the crystal lamellae and preferentially segregated at the eyes and boundaries of the spherilities.[9b] TPE is much larger than these end groups and should have a higher chance to be residing on the surface of PCL-TPE crystals, as schematically illustrated in Scheme 1.

Taking advantage of pendant TPE moieties on surface, PCL-TPE nanosheets were used to detect explosives. PCL-TPE nanosheets suspended in aqueous media emitted efficiently upon radiation at 365 nm. With addition of picric acid (PA), emission decreased gradually. The value of I_0/I decreased lineally with increasing PA concentration (Figure 4).

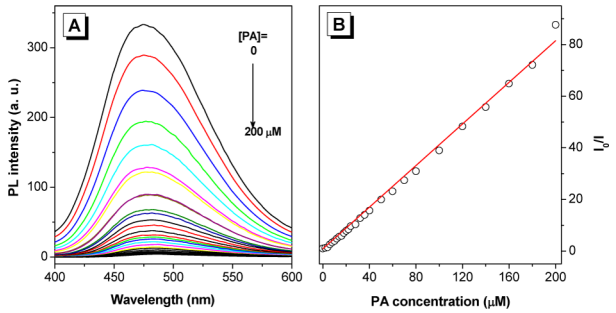

Figure 4. (A) PL spectra of PCL-TPE nanosheets suspension containing various amount of picric acid (PA) and (B) plots of I_0/I values vs PA concentrations in PCL-TPE suspension. The static quenching constant (K) was 380000 L mol^{-1} for PCL-TPE nanosheets.

Quenching of PCL-TPE with picric acid followed the Stern–Volmer relation:

$$I_0/I = 1 + K[Q] \quad (1)$$

where I_0 and I are the steady-state fluorescence intensities in the absence and in the presence of quencher, respectively. K denotes the Stern–Volmer constant, which represents the sensitivity of fluorescent material toward quencher. Larger K values mean higher sensitivity toward analysts. The value of K was determined to be 380000 L mol^{-1} for PCL-TPE nanosheets, by far larger than those of the bare TPE (K = 48700 L/mol, Figure S17) and fluorescent chemosensors based on polysiloles (K < 20000 L/mol).[12] This means that PCL-TPE nanosheets are by far sensitive against PA as compared to bare TPE and conventional polysiloles. The high static quenching constant (K) of PCL-TPE is presumably related to the novel structure of nanosheets where fluorescence TPE moieties are coated on the surface.

We next investigated the fluorescence response of PCL-TPE nanosheets to explosive analogues. Blank PCL-TPE emitted strong blue light under radiation at 365 nm. Addition of equivalent mole of PA resulted in quenching of its blue emission. While in the presence of an equivalent mole of PA analogues, such as toluene (Tol), 2,4-dinitrotolene (DNT), 4-nitrophenol (NP), 4-nitrobenzol (NB), 2-bromotoluene (BT), 1,2-dichlorobenzene (DCB), 1,2,4-tribromobenzene (TBB), bromo-2-nitrobenzene (BNB), and 3,5-dinitrobenzl alcohol (DNBA), emission of PCL-TPE suspension still can be observed by naked eyes. The values of I_0/I of PCL-TPE in the presence of PA and its analogues were summarized in Figure 5. PA showed by far larger I_0/I value, revealing that PCL-TPE nanosheets exhibited superior specificity toward PA against its analogues.

We investigated the effect of molecular weight of PCL-TPE on quenching constant (K). The values of K decreased with increasing molecular weight of PCL-TPE (Figures S18–S21, SI). A possible reason is that grafting density of TPE on PCL lamellae is related to the molecular weight of PCL-TPE. PCL-TPE with low molecular weight forms fluorescent nanosheets with high TPE grafting density due to high TPE fraction. In the presence of PA, a PA molecule quenches the emission of

dx.doi.org/10.1021/mz4005887 | ACS Macro Lett. 2014, 3, 21–25

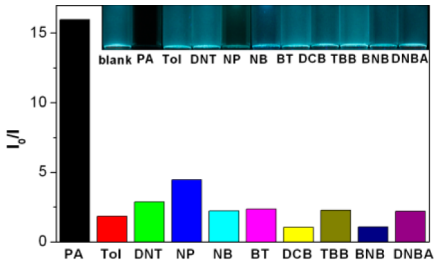

Figure 5. Variation of fluorescence intensity (I_0/I) of PCL-TPE with addition of picric acid (PA), toluene (Tol), 2,4-dinitrotolene (DNT), 4-nitrophenol (NP), 4-nitrobenzol (NB), 2-bromotoluene (BT), 1,2-dichlorobenzene (DCB), 1,2,4-tribromobenzene (TBB), bromo-2-nitrobenzene (BNB), 3,5-dinitrobenzl alcohol (DNBA). Inset showed the digital images of PCL-TPE suspension with various explosive analogues.

several adjacent TPE molecules, resulting in high detection sensitivity. For PCL-TPE with high molecular weight, TPE moieties reside individually and isolatedly on the surface of polymeric lamellae due to low TPE fraction. To quench the emission of the individual TPE molecules, more PA molecules are required, leading to low quenching constant.

In summary, fluorescent nanosheets were generated by crystallization of polymers capped with tetraphenylethene (TPE) moieties. During crystallization of polymers, TPE moieties were expelled out of lamellar crystal of polymers, and finally pended on the surface of nanosheets. Fluorescent nanosheets with dangling TPE molecules showed sensitive and specific response to model explosives of picric acid. Such polymer crystallization-induced fluorescent nanomaterials offers a new avenue to functional nanomaterials with potential applications in nanodevices, biological engineering, and so on.

■ ASSOCIATED CONTENT

Supporting Information

Materials and instruments, synthesis and characterization of the PCL-TPE, and NMR, mass, DSC, XRD, and XPS spectra are supplied. This material is available free of charge via the Internet at http://pubs.acs.org.

■ AUTHOR INFORMATION

Corresponding Author

*E-mail: tangbenz@ust.hk.

Notes

The authors declare no competing financial interest.

■ ACKNOWLEDGMENTS

This work was partially supported by the National Basic Research Program of China (973 Program; 2013CB834701), the Research Grants Council of Hong Kong (HKUST2/CRF/10 and N_HKUST620/11) and the University Grants Committee of Hong Kong (AoE/P-03/08). B.Z.T. thanks the support from Guangdong Innovative Research Team Program of China (201101C0105067115) and G.D.L thanks the support from the Hong Kong Scholar Program (XJ2011047), NSFC (21374136 and 21074151), and The Fundamental Research Funds for the Central Universities (13lgzd04).

■ REFERENCES

(1) (a) Hong, Y. N.; Lam, J. W. Y.; Tang, B. Z. *Chem. Soc. Rev.* **2011**, *40*, 5361−5388. (b) Yuan, W. Z.; Tan, Y. Q.; Gong, Y. Y.; Lu, P.; Lam, J. W. Y.; Shen, X. Y.; Feng, C. F.; Sung, H. H. Y.; Lu, Y. W.; Williams, I. D.; Sun, J. Z.; Zhang, Y. M.; Tang, B. Z. *Adv. Mater.* **2013**, *25*, 2837−2843. (c) Wang, Z. K.; Chen, S. J.; Lam, J. W. Y.; Qin, W.; Kwok, R. T. K.; Xie, N.; Hu, Q. L.; Tang, B. Z. *J. Am. Chem. Soc.* **2013**, *135*, 8238−8245. (d) Leung, C. W. T.; Hong, Y. N.; Chen, S. J.; Zhao, E. G.; Lam, J. W. Y.; Tang, B. Z. *J. Am. Chem. Soc.* **2013**, *135*, 62−65. (e) Chen, S. J.; Hong, Y. N.; Liu, Y.; Liu, J. Z.; Leung, C. W. T.; Li, M.; Kwok, R. T. K.; Zhao, E. G.; Lam, J. W. Y.; Yu, Y.; Tang, B. Z. *J. Am. Chem. Soc.* **2013**, *135*, 4926−4929.

(2) (a) Yuan, W. Z.; Mahtab, F.; Gong, Y. Y.; Yu, Z. Q.; Lu, P.; Tang, Y. H.; Lam, J. W. Y.; Zhu, C. Z.; Tang, B. Z. *J. Mater. Chem.* **2012**, *22*, 10472−10479. (b) Zhao, Z. J.; Liu, D. D.; Mahtab, F.; Xin, L. Y.; Shen, Z. F.; Yu, Y.; Chan, C. Y. K.; Lu, P.; Lam, J. W. Y.; Sung, H. H. Y.; Williams, I. D.; Yang, B.; Ma, Y. G.; Tang, B. Z. *Chem.—Eur. J.* **2011**, *17*, 5998−6008. (c) Wang, W. H.; Wang, S. Y.; Hong, Y. N.; Tang, B. Z.; Lin, N. *Chem. Commun.* **2011**, *47*, 10073−10075. (d) Zhao, Z. J.; Chen, S. M.; Shen, X. Y.; Mahtab, F.; Yu, Y.; Lu, P.; Lam, J. W. Y.; Kwok, H. S.; Tang, B. Z. *Chem. Commun.* **2010**, *46*, 686−688.

(3) (a) Luo, X. L.; Li, J. N.; Li, C. H.; Heng, L. P.; Dong, Y. Q.; Liu, Z. P.; Bo, Z. S.; Tang, B. Z. *Adv. Mater.* **2011**, *23*, 3261−3265. (b) Gu, X. G.; Yao, J. J.; Zhang, G. X.; Yan, Y. L.; Zhang, C.; Peng, Q.; Liao, Q.; Wu, Y. S.; Xu, Z. Z.; Zhao, Y. S.; Fu, H. B.; Zhang, D. Q. *Adv. Funct. Mater.* **2012**, *22*, 4862−4872. (c) Gu, X. G.; Yao, J. J.; Zhang, G. X.; Zhang, D. Q. *Small* **2012**, *8*, 3406−3411.

(4) (a) He, W. N.; Xu, J. T. *Prog. Polym. Sci.* **2012**, *37*, 1350−1400. (b) Dong, B.; Li, B.; Li, C. Y. *J. Mater. Chem.* **2011**, *21*, 13155−13158. (c) Wang, B. B.; Li, B.; Ferrier, R. C. M.; Li, C. Y. *Macromol. Rapid Commun.* **2010**, *31*, 169−175. (d) Bao, S. P.; Liu, T. T.; Liang, G. D.; Gao, H. Y.; Zhu, F. M.; Wu, Q. *Chem.—Eur. J.* **2012**, *18*, 15272−15276.

(5) (a) Wu, P.; Yan, X. P. *Chem. Soc. Rev.* **2013**, *42*, 5489−5521. (b) Maldonado, C. R.; Salassa, L.; Gomez-Blanco, N.; Mareque−Rivas, J. C. *Coord. Chem. Rev.* **2013**, *257*, 2668−2688. (c) Schulz, A.; McDonagh, C. *Soft Matter* **2012**, *8*, 2579−2585. (d) Schladt, T. D.; Schneider, K.; Schild, H.; Tremel, W. *Dalton Trans.* **2011**, *40*, 6315−6343.

(6) (a) Cipitria, A.; Skelton, A.; Dargaville, T. R.; Dalton, P. D.; Hutmacher, D. W. *J. Mater. Chem.* **2011**, *21*, 9419−9453. (b) Luk, J. Z.; Cooper-White, J.; Rintoul, L.; Taran, E.; Grondahl, L. *J. Mater. Chem. B* **2013**, *1*, 4171−4181. (c) Zhou, B.; Tong, Z. Z.; Huang, J.; Xu, J. T.; Fan, Z. Q. *CrystEngComm* **2013**, *15*, 7824−7832.

(7) (a) Xu, B. J.; Xie, M. Y.; He, J. J.; Xu, B.; Chi, Z. G.; Tian, W. J.; Jiang, L.; Zhao, F. L.; Liu, S. W.; Zhang, Y.; Xu, Z. Z.; Xu, J. R. *Chem. Commun.* **2013**, *49*, 273−275. (b) Liu, X. H.; Jiao, J. M.; Jiang, X. X.; Li, J. F.; Cheng, Y. X.; Zhu, C. J. *J. Mater. Chem. C* **2013**, *1*, 4713−4719. (c) Baglan, M.; Atilgan, S. *Chem. Commun.* **2013**, *49*, 5325−5327.

(8) (a) Mareau, V. H.; Prud'homme, R. E. *Macromolecules* **2005**, *38*, 398−408. (b) Sanandaji, N.; Ovaskainen, L.; Gunnewiek, M. K.; Vancso, G. J.; Hedenqvist, M. S.; Yu, S.; Eriksson, L.; Roth, S. V.; Gedde, U. W. *Polymer* **2013**, *54*, 1497−1503.

(9) (a) Delcorte, A. Fundamentals of organic SIMS: insights from experiments to models. In *ToF-SIMS: Materials Analysis by Mass Spectrometry*, 2nd ed.; Vickerman, J.C., Briggs, D., Eds.; IM Publications and Surface Spectra Limited: Chichester, 2013; pp 87−123. (b) Weng, L. T.; Chan, C. M. Characterization of polymeric materials. In *ToF-SIMS: Materials Analysis by Mass Spectrometry*, 2nd ed.; Vickerman, J.C., Briggs, D., Eds.; IM Publications and Surface Spectra Limited: Chichester, 2013; pp 503−530. (c) Weng, L. T.; Chan, C. M. Surface analysis. In *Wiley Encyclopedia of Composites*, 2nd ed.; Nicolais, L., Borzacchiello, A., Lee, S. M., Eds.; Wiley: Chichester, 2012; pp2974−2993.

(10) Hu, H. L.; Dorset, D. L. *Macromolecules* **1990**, *23*, 4604−4607.

(11) (a) Wang, B. B.; Li, B.; Zhao, B.; Li, C. Y. *J. Am. Chem. Soc.* **2008**, *130*, 11594−11595. (b) Cheng, S. Z. D.; Wu, S. S.; Chen, J. H.; Zhuo, Q. H.; Quirk, R. P.; Vonmeerwall, E. D.; Hsiao, B. S.; Habenschuss, A.; Zschack, P. R. *Macromolecules* **1993**, *26*, 5105−5117.

(12) (a) Sanchez, J. C.; DiPasquale, A. G.; Rheingold, A. L.; Trogler, W. C. *Chem. Mater.* **2007**, *19*, 6459−6470. (b) Liu, J. Z.; Zhong, Y. C.; Lam, J. W. Y.; Lu, P.; Hong, Y. N.; Yu, Y.; Yue, Y. N.; Faisal, M.; Sung,

H. H. Y.; Williams, I. D.; Wong, K. S.; Tang, B. Z. *Macromolecules* **2010**, *43*, 4921−4936.